www.czasopisma.pan.pl PAN POLSKA AKADEMIA NAUK www.journals.pan.pl

Arch. Metall. Mater. **67** (2022), 2, 685-690

DOI: https://doi.org/10.24425/amm.2022.137806

MUHAMMAD RAZLAN ZAKARIA[1,2], MOHD FIRDAUS OMAR[1,2*], HAZIZAN MD AKIL[3], MUHAMMAD BISYRUL HAFI OTHMAN[4], MOHD MUSTAFA AL BAKRI ABDULLAH[1,2]

ENHANCEMENT OF TENSILE PROPERTIES OF GLASS FIBRE EPOXY LAMINATED COMPOSITES REINFORCED WITH CARBON NANOTUBES INTERLAYER USING ELECTROSPRAY DEPOSITION

The introduction of carbon nanotubes (CNTs) onto glass fibre (GF) to create a hierarchical structure of epoxy laminated composites has attracted considerable interest due to their merits in improving performance and multifunctionality. Field emission scanning electron microscopy (FESEM) was used to analyze the woven hybrid GF-CNT. The results demonstrated that CNT was successfully deposited on the woven GF surface. Woven hybrid GF-CNT epoxy laminated composites were then prepared and compared with woven GF epoxy laminated composites in terms of their tensile properties. The results indicated that the tensile strength and tensile modulus of the woven hybrid GF-CNT epoxy laminated composites were improved by up to 9% and 8%, respectively compared to the woven hybrid GF epoxy laminated composites.

Keywords: Glass fibre; Carbon Nanotubes; Hybrid Material; Epoxy Laminated Composites

1. Introduction

Advanced fibre reinforced polymer composites (FRPs) are considered to have superior performance and continue to be used in many structural applications [1]. FRPs have been used magnificently in numerous fields, such as aerospace, military, construction and automotive, due to their remarkable properties, including low weight, high strength , high stiffness, corrosion resistance and multi-functionality, making them attractive compared to other conventional materials [2]. However, most FRPs are prone to micro and nano damage, such as fibre breakage, matrix cracking and interfacial debonding [3]. As such, a composite made from a well-suited matrix and strong fibre cannot inherently produce a strong material since the fibre/matrix interface is equally critical in deciding the final performance of the composites [4].

Carbon nanotubes (CNTs) have remarkable mechanical and physical properties, such as high modulus and strength, making them the perfect reinforcement for polymer composites [5-10]. In the last decade, the introduction of CNTs onto traditional fibres to construct a hierarchical reinforcement system in polymer composites has brought considerable interest to the implementation of the successful “bridge” of the fibre/matrix interface [11]. To date, few methods, such as chemical vapour deposition (CVD) [12-16], electrophoretic deposition (EPD) [17-19] and chemical functionalization [20-22], have been developed primarily to prepare multiscale hybrid CNT-fibres. Such approaches have been shown to efficiently enhance the fibre-matrix interface, which in turn improves the mechanical properties of hierarchical polymer composites [23]. However, there are still some disadvantages and limitations on the basis of these methods. The CVD method has an advantage in terms of controlled growth and dispersion of CNTs on the surface of the fibre [24]. Whereas during the CVD process, the use of high temperatures will impose significant drawbacks such as fibre degradation and scalability [25].

Meanwhile, the EPD method demonstrates promising and potential in terms of scalability, cost-effectiveness and practicality [26]. Previously, carbon fibre was used in the centre of the two metallic electrodes as the deposition electrode and the hybrid GF-CNT were continuously prepared [17]. In contrast to CF, glass fibre (GF) cannot be used as a deposition electrode directly because of its insulating properties. Zhang et al. attempted to create a hybrid GF-CNT by using two parallel copper plates for cathode and anode [27]. However, the results showed that the

[1] UNIVERSITI MALAYSIA PERLIS (UNIMAP), FACULTY OF CHEMICAL ENGINEERING TECHNOLOGY PERLIS, MALAYSIA
[2] UNIVERSITI MALAYSIA PERLIS (UNIMAP), GEOPOLYMER & GREEN TECHNOLOGY, CENTRE OF EXCELLENT (CEGEOGTECH), PERLIS, MALAYSIA
[3] UNIVERSITI SAINS MALAYSIA, SCHOOL OF MATERIALS AND MINERAL RESOURCES ENGINEERING, ENGINEERING CAMPUS, 14300 NIBONG TEBAL, PULAU PINANG, MALAYSIA
[4] UNIVERSITI SAINS MALAYSIA, SCHOOL OF CHEMICAL SCIENCES, 11800 MINDEN, PENANG, MALAYSIA

* Corresponding author: firdausomar@unimap.edu.my

EPD method was still very difficult to achieve a homogeneous distribution of the CNT on the surface of the GF [28]. In addition, the EPD method also has similar disadvantages with the chemical functionalization method, which both expose CNT to oxidation. This oxidation treatment can damage the structure of CNT and can contribute to the degradation of the mechanical properties polymer composites.

Electrospray is another one of the most promising manipulation method for the deposit of nano-materials and has been used on an industrial scale in agriculture, sanitization and sensor fields [25]. Electrospray is a simple, cost-effective method where a liquid or suspension is made into a fine aerosol and directed onto a target surface using an electric field [23]. In addition, the motion of the CNT can be easily controlled by the electrical field and the agglomeration of the CNT can be prevented.

In this paper, preparation of woven hybrid GF-CNT was developed through a ESD method. The woven hybrid GF-CNT that was produced using this method was characterized by field emission scanning electron microscopy (FESEM). Then, woven hybrid GF-CNT epoxy laminated composites were fabricated using vacuum-assisted resin transfer moulding to produce samples with a good finish to ensure the reliability of the test. The tensile properties of woven hybrid GF-CNT epoxy laminated composites were measured to evaluate the reinforcing effect of the woven hybrid GF-CNT. Finally, the microscopic morphologies and fracture behaviours of the woven hybrid GF-CNT epoxy laminated composites were characterized and discussed.

2. Experimental

Industrial grade multi-walled carbon nanotubes (MWCNTs) was purchased from SkySpring Nanomaterials Inc. and used as received. The MWCNTs have a purity of 99.5 wt%, length in the range of 5-30 μm, outside diameter 10-20 nm and inside diameter 3-5 nm. Woven 'E' GF with size of 400 gsm was purchased at CL Composites Sdn.Bhd. The epoxy resins DER 331 and Epoxy Hardener Clear were supplied by Euro Chemo Pharma Sdn.Bhd. The solvent N,N-dimethylformamide (DMF) was purchased from Sigma-Aldrich.

In order to prepare the CNT dispersion, 0.005 g CNTs were dispersed in 5 ml of the DMF by using sonicator at a frequency of 50 kHz for 30 minutes. In order to improve attachment strength of CNT onto GF surface, the epoxy resin DER 331 was mixed with the Epoxy Hardener Clear at 10:6 by weight ratio. Then, 0.003 g of the resulting mixture was added to a CNT dispersion and ultrasonicated for another 30 minutes.

In order to prepare for electrospray, the equipment consists of a stainless-steel needle (with 0.3 mm inner diameter and 0.55 mm outer diameter) and a steel platform as a ground electrode. The precision high voltage power supply (Model type ES20P-20W) which capable of delivering an applied voltage of 20 kV with a resolution of 0.1 kV is connected to the stainless-steel needle (with 0.3 mm inner diameter and 0.55 mm outer diameter). The needle is fitted to a syringe of 20 ml and the syringe sits firmly on a precision syringe pump (Model type NE-1600, New Era Pump Systems, Inc., USA), which can deliver low flow rates up to 0.001 μL/hr. Woven GF fixed onto the roller and the steel platform connected with an earth wire. The electrospray deposition process was then carried out as explained. By rotating the roller at 120 rpm, the woven GF was sprayed by turn to achieve an even deposition and coating. The distance between the needle and roller was fixed to be 10 cm, and the flow rate was 0.02 ml/hr with different applied voltage from 2 kV to 20 kV. On completion of the spray process, the woven GF was left to dry for 24 hours, and the spray process was repeated on the opposite side. Fig. 1 shows a general view of the electrospray deposition setup.

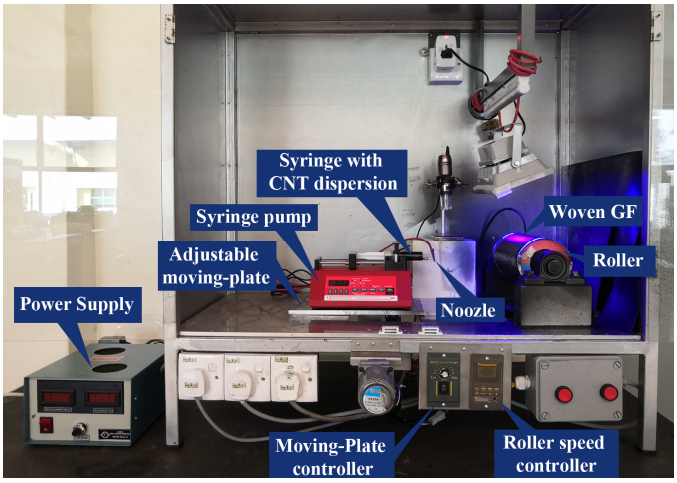

Fig. 1. General view of electrospray deposition process

An field emission scanning electron microscope (FESEM) (ZEISS Supra 55 SEM VP) was used to analyse the morphology of the woven hybrid GF-CNT. The woven hybrid GF-CNT was coated with a thin layer of gold to improve their conductance for observations using FESEM.

Vacuum assisted Resin Transfer Moulding (VARTM) was used to prepare the woven hybrid GF-CNT epoxy laminated composited. In this case, the woven hybrid GF-CNT was selected based on the optimum voltage to produce uniform CNT coating on the woven CF. Three layers of woven hybrid GF-CNT were then stacked together inside the mould cavity to form a 2.5 mm thick plate. The EpoxAmite 100 resin and EpoxAmite 103 slow hardener were prepared by mixing them at a mass ratio of 100:28.4. A vacuum was applied to the mould to provide the required pressure to force the epoxy suspension into the preform. The vacuum pump was left running during the process, which lasted for about 20 minutes, to facilitate the infiltration of the epoxy suspension. After the mould had been fully infiltrated with the epoxy suspension, both the inlet and outlet were closed and maintained under a constant vacuum of 75 cmHg. The vacuum was discontinued after the epoxy suspension had been cured and the woven hybrid GF-CNT epoxy laminated composites part had been de-moulded. The same process was used to prepare woven GF epoxy laminated composites. The description of the samples is given in Table 1.

TABLE 1

Description of the samples

Sample	Description
Epoxy/GF	Epoxy reinforced with 3 layers of woven GF
Epoxy/GF/CNTs	Epoxy reinforced with 3 layers of woven hybrid GF-CNT

The tensile properties of Epoxy/GF and Epoxy/GF/CNTs were measured using a universal testing machine (Model: 5982, Instron, USA) according to ASTM D3039. The tensile test samples were cut from the Epoxy/GF and Epoxy/GF/CNTs panels with dimension of 250 mm (length) × 25 mm (width) × 2.5 mm (thickness). For this purpose, the crosshead speed of 2.0 mm/min was used. For each case, at least five specimens were tested to ensure the test results were reliable. The fracture surface of the tensile specimen was coated with a thin layer of gold and observed using SEM.

3. Results and discussion

The surface morphologies of the CNT, GF and hybrid GF-CNT were characterized by using FESEM. Fig. 2a-b shows the morphological structure of the CNT in the form of tubular with diameter about 10-20 nm. Based on the observation, it can be seen CNT tends to agglomerate due to Van der Waals force. Fig. 2c-d displays the morphological structure of the GF with diameter about 13 μm. In addition, the smooth surface of GF along their axis also can be clearly seen.

Fig. 3 shows the SEM images of hybrid GF-CNT produced as a function of varying voltage. Fig. 3a-b show the morphologies of the hybrid GF-CNT produced at voltage 8 kV. From the observation, it can be seen that the CNT did not completely cover the entire surface of GF. At low applied voltage of 8 kV, the size of the droplets is large and the solvent evaporation rate is slow. This is because the greater amount of solvent remained in each droplet until it hit the surface of the fibre. Therefore, a longer travel time is needed to completely eliminate this solvent by evaporation. As a result, large droplets with an accumulation of CNT will not hit the surface of glass fibre, resulting in a loss of CNT. Further increasing the applied voltage lowers the percentage of the CNT aggregate. Fig. 3c-d show the morphologies of the hybrid GF-CNT produced at voltage 13 kV. From the observation, it can be seen that the most CNT deposited on the surface of GF. At voltage of 18 kV, the density of CNT deposited on the GF surface decreased as shown in Fig. 3e-f.

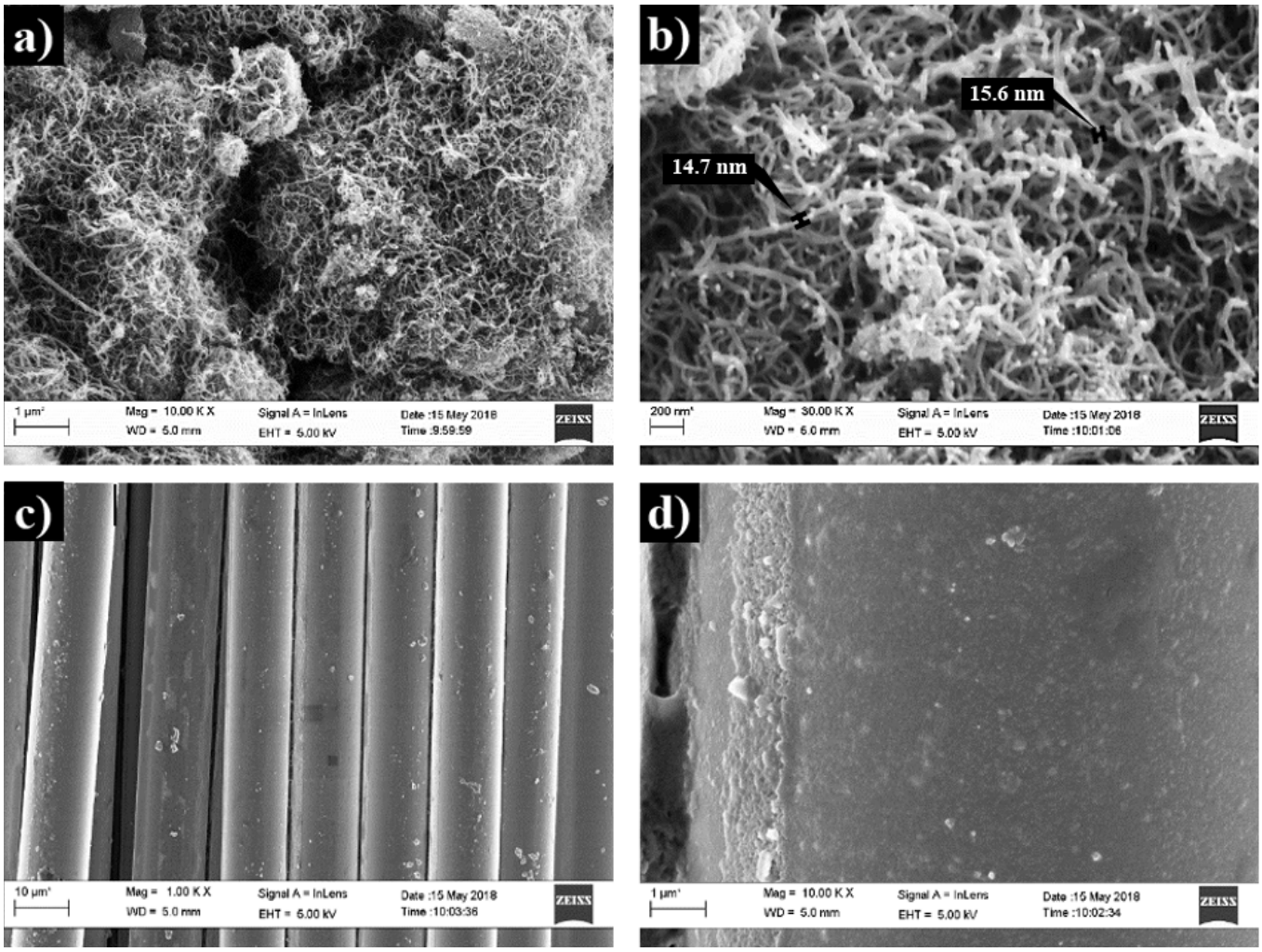

Fig. 2. SEM images of (a-b) CNT and (c-d) GF

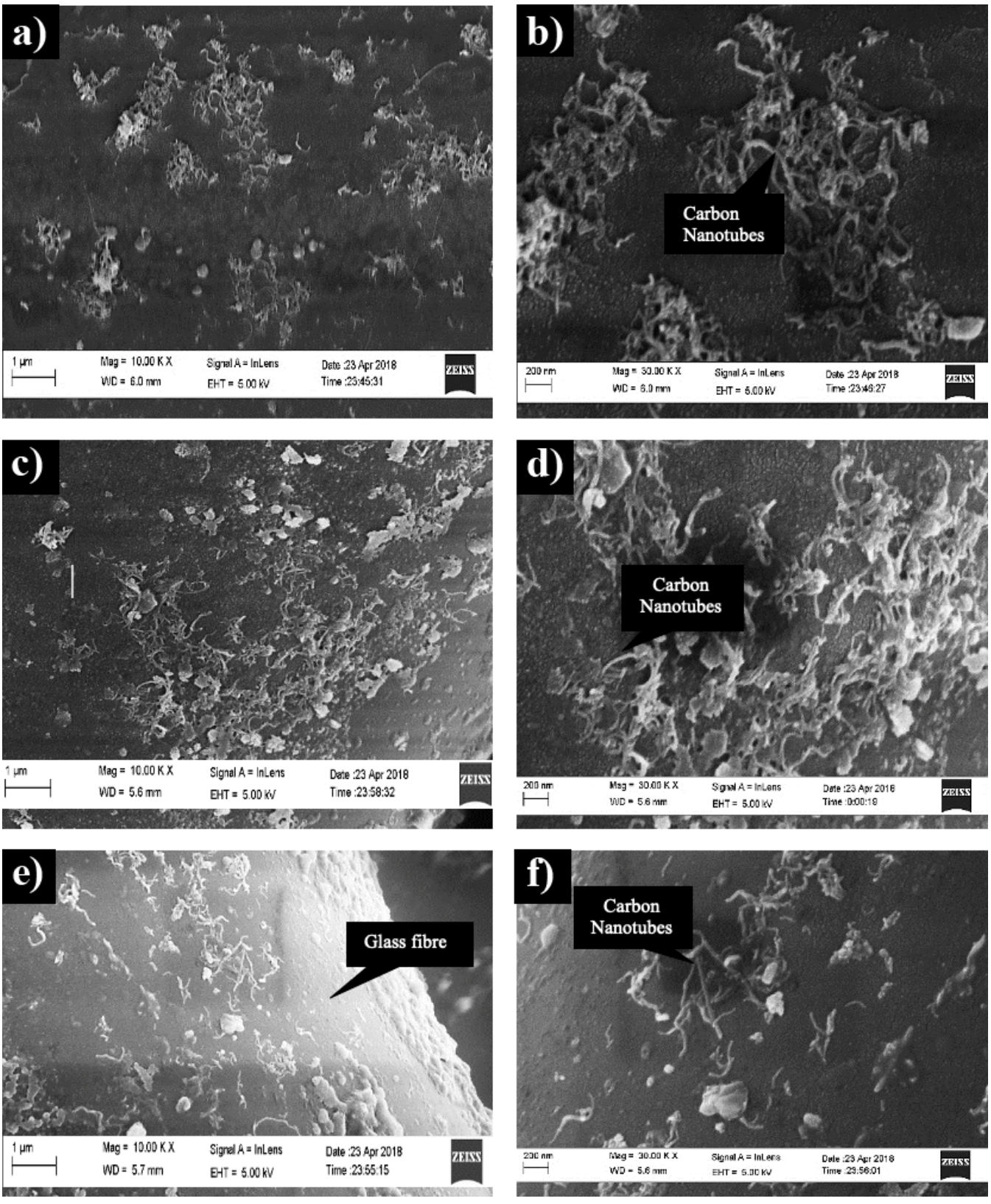

Fig. 3. SEM images of hybrid GF-CNT produced at applied voltage of (a-b) 8 kV, (c-d) 13 kV and (e-f) 18 kV

This is due to increases in applied voltage will enlarge the spray area and cause the waste of CNT. This is due to an increase in the applied voltage, which will enlarge the spray area and cause waste of CNT. From the morphological observation of the GF-CNT hybrid at various applied voltages, it was found that the optimum CNT deposition on the GF surface was at an applied voltage of 13 kV.

Tensile tests were carried out to determine the effect of CNT on the tensile properties of Epoxy/ GF/ CNTs and Epoxy/GF, which served as a control sample. Typical tensile stress-strain

curves of the tensile test were shown in Fig. 4. From the result, it can be seen Epoxy/GF/CNTs shows a relatively higher tensile stress while Epoxy/GF shows a higher tensile strain. Fig. 5 shows the average tensile strength and tensile modulus obtained from this stress-strain curve. As can be seen, the Epoxy/GF/CNTs showed a higher tensile strength and tensile modulus compared to Epoxy/GF. The highest average UTS is achieved by the Epoxy/GF/CNTs with an increment of up to about 6.70 MPa which corresponds to an 9% increment compared to the Epoxy/GF. The explanation for this increase in UTS is due to a better distribution of CNT on the GF surface, improved interfacial bonding leads to an improvement in the interfacial strength between CNT and fibre and results in an effective transfer of stress between CNT and fibre. From Fig. 5b, a similar trend for the tensile modulus is also observed. The Epoxy/GF/CNTs showed that the higher tensile modulus was achieved by an increase of 8%, which is 2.37 GPa compared to the Epoxy/GF of 2.21 GPa. Generally, an increase in the modulus can be achieved by adding fillers such as CNT. The presence of the CNT results in an increase in resistance to deformation, which subsequently increases the stiffness of the Epoxy/ GF/CNTs. The reason that this tensile modulus is similar trend to the tensile strength is due to the uniform distribution of CNT on the surface of CF. For the fracture strain, it can be seen the fracture strain of the Epoxy/GF/CNTs lower than Epoxy/GF. This is due to the addition of the CNT resulting in increased rigidity

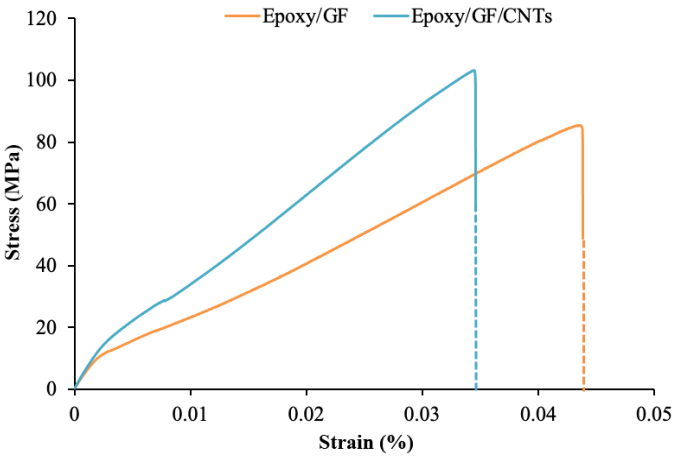

Fig. 4. Tensile stress-strain curves of Epoxy/GF and Epoxy/ GF/ CNTs

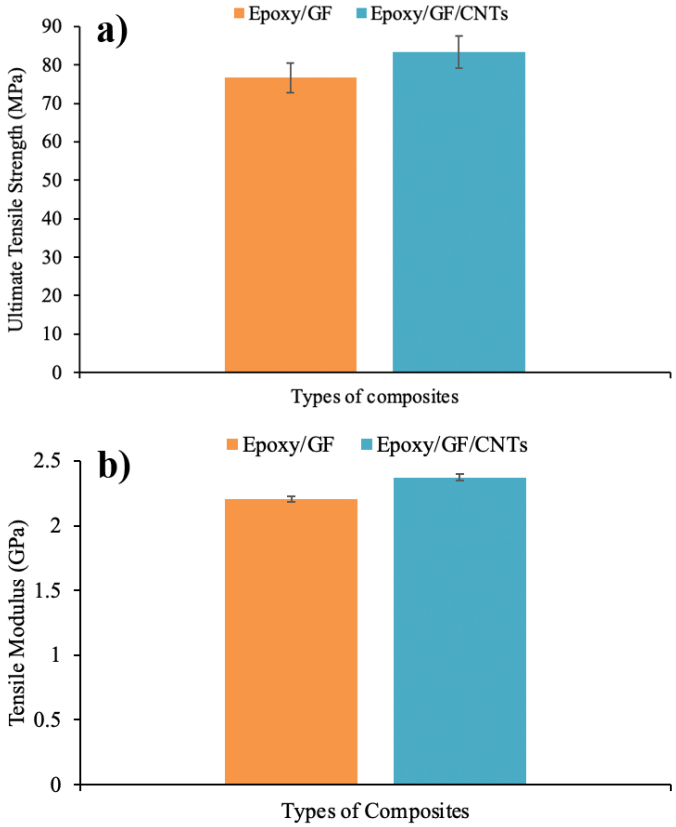

Fig. 5. Tensile properties of the Epoxy/GF and Epoxy/ GF/ CNTs (a) ultimate tensile strength and (b) tensile modulus

Fig. 6 show the morphologies of the tensile fractured surface of the Epoxy/GF and Epoxy/ GF/ CNTs. From the Fig. 6a, Epoxy/GF demonstrated a clean and smooth fibre-matrix interface fracture. Meanwhile, Fig. 6b demonstrated that epoxy resin remains attached to the fibre for Epoxy/ GF/ CNTs. Thus, the deposit of CNT on GF can be seen to help create local mechanical interlocking within the matrix and fibre, which also increases the frictional force at the interface.

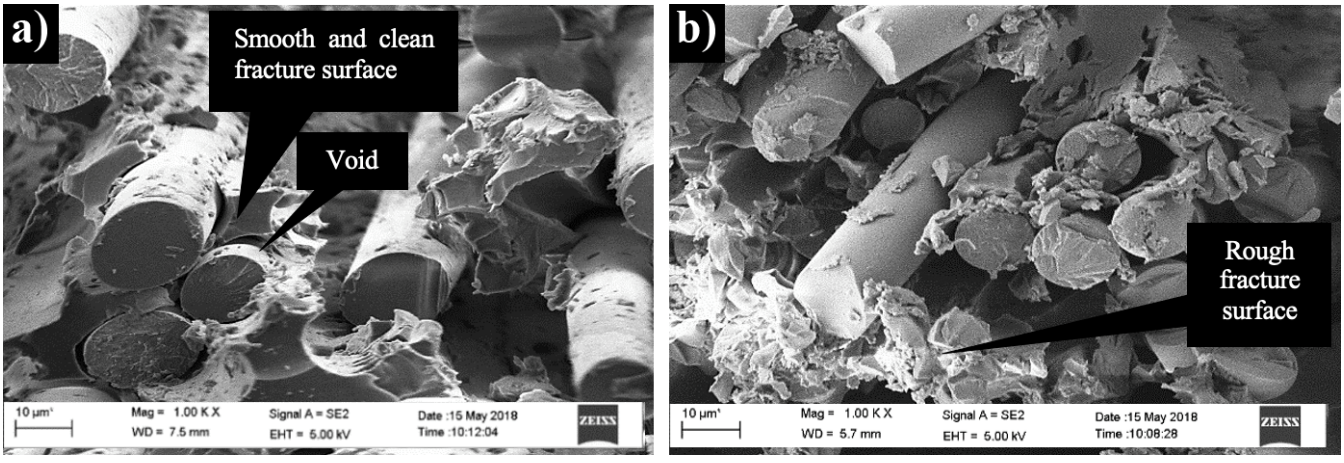

Fig. 6. SEM images of the fracture surfaces of (a) Epoxy/GF and (b) Epoxy/ GF/ CNTs

4. Conclusion

This study demonstrated that the electrospray deposition (ESD) method can be used to produce woven hybrid GF-CNT. The FESEM results proved that the final morphology of woven hybrid GF-CNT was found to be strongly influenced by applied voltage. Based on the experimental results, it can be concluded that the optimized voltage to deposit CNT on the woven CF surface is 15 kV. The woven hybrid GF-CNT epoxy laminated composites have demonstrated higher tensile properties compared to woven GF epoxy laminated composites. The tensile strength and tensile modulus of the woven hybrid GF-CNT epoxy laminated composites were enhanced by about 9% and 8%, respectively compared to the woven GF epoxy laminated composites. This improvement is due to the presence of CNT on the woven GF surface and significantly improving the load transfer in epoxy laminated composites.

Acknowledgements

The authors would like to acknowledge Universiti Sains Malaysia (USM) RUI 1001/PBAHAN/8014047 for sponsoring and providing financial assistance during this research work and Universiti Malaysia Perlis for sponsoring postdoctoral fellowship.

REFERENCES

[1] A.I. Selmy, N.A. Azab, M.A. Abd El-baky, Composites Part B: Engineering **45** (1), 518-527 (2013).
[2] G. Zhao, H.-Y. Liu, X. Du, H. Zhou, Z. Pan, Y.-W. Mai, Y.-Y. Jia, W. Yan, Composites Part B: Engineering **198**, 108249 (2020).
[3] L. Tzounis, M. Zappalorto, F. Panozzo, K. Tsirka, L. Maragoni, A.S. Paipetis, M. Quaresimin, Composites Part B: Engineering **169**, 37-44 (2019).
[4] A.F.M. Nor, M.T.H. Sultan, M. Jawaid, A.M.R. Azmi, A.U.M. Shah, Composites Part B: Engineering **168**, 166-174 (2019).
[5] M.R. Zakaria, M.H. Abdul Kudus, H. Md. Akil, M.Z. Mohd Thirmizir, Composites Part B: Engineering **119**, 57-66 (2017).
[6] M.R. Zakaria, M.H. Abdul Kudus, H. Md Akil, M.Z.M. Thirmizir, M.F.I. Abdul Malik, M.B.H. Othman, F. Ullah, F. Javed, Polymer Composites **40** (S2), E1840-E1849 (2019).
[7] M.R. Zakaria, H.M. Akil, M.H.A. Kudus, S.S.M. Saleh, Composites Part A: Applied Science and Manufacturing **66**, 109-116 (2014).
[8] M.R. Zakaria, H. Md. Akil, M.H. Abdul Kudus, A.H. Kadarman, Composite Structures **132**, 50-64 (2015).
[9] M.R. Zakaria, M.H. Abdul Kudus, H. Md. Akil, M.H. Zamri, Materials **10** (3) (2017).
[10] C.L. Han, G.-D. Wang, N. Li, M. Wang, X.l. Liu, J.h. Ma, Composite Structures **272**, 114191 (2021).
[11] Y. Wu, D. Dhamodharan, Z. Wang, R. Wang, L. Wu, Composites Part B: Engineering **195**, 108093 (2020).
[12] X. Xu, J. Zhou, L. Jiang, G. Lubineau, S.A. Payne, D. Gutschmidt, Carbon **80**, 91-102 (2014).
[13] Z.-G. Zhao, L.-J. Ci, H.-M. Cheng, J.-B. Bai, Carbon **43** (3), 663-665 (2005).
[14] A.Y. Boroujeni, M. Tehrani, A.J. Nelson, M. Al-Haik, Composites Part B: Engineering **66**, 475-483 (2014).
[15] K.L. Kepple, G.P. Sanborn, P.A. Lacasse, K.M. Gruenberg, W.J. Ready, Carbon **46** (15), 2026-2033 (2008).
[16] P. Lv, Y.-y. Feng, P. Zhang, H.-m. Chen, N. Zhao, W. Feng, Carbon **49** (14), 4665-4673 (2011).
[17] J. Guo,C. Lu, Carbon **50** (8), 3101-3103 (2012).
[18] X. Yao, X. Gao, J. Jiang, C. Xu, C. Deng, J. Wang, Composites Part B: Engineering **132**, 170-177 (2018).
[19] Y.J. Kwon, Y. Kim, H. Jeon, S. Cho, W. Lee, J.U. Lee, Composites Part B: Engineering **122**, 23-30 (2017).
[20] W. Zhang, X. Deng, G. Sui, X. Yang, Carbon **145**, 629-639 (2019).
[21] G. Wu, L. Ma, L. Liu, Y. Wang, F. Xie, Z. Zhong, M. Zhao, B. Jiang, Y. Huang, Composites Part B: Engineering **82**, 50-58 (2015).
[22] M. Li, Y. Gu, Y. Liu, Y. Li, Z. Zhang, Carbon **52**, 109-121 (2013).
[23] M.R. Zakaria, H. Md Akil, M.H. Abdul Kudus, F. Ullah, F. Javed, N. Nosbi, Composites Part B: Engineering **176**, 107313 (2019).
[24] T.R. Pozegic, I. Hamerton, J.V. Anguita, W. Tang, P. Ballocchi, P. Jenkins, S.R.P. Silva, Carbon **74**, 319-328 (2014).
[25] Q. Li, J.S. Church, M. Naebe, B.L. Fox, Carbon **109**, 74-86 (2016).
[26] N. M.S., R. K.V., S.K. P., F.K. P., V. P., J. K., Chemical Engineering and Processing – Process Intensification **160**, 108298 (2021).
[27] J. Zhang, R. Zhuang, J. Liu, E. Mäder, G. Heinrich, S. Gao, Carbon **48** (8), 2273-2281 (2010).
[28] H. Dai, E.T. Thostenson, T. Schumacher, Composites Part B: Engineering **222**, 109068 (2021).